Nuclear Materials and Energy 24 (2020) 100754

Contents lists available at ScienceDirect

Nuclear Materials and Energy

journal homepage: www.elsevier.com/locate/nme

Microstructure and mechanical properties of hot rolled ODS copper

A. Muñoz[a,*], B. Savoini[a], M.A. Monge[a], M. Eddahbi[a], O.J. Dura[b]

[a] Universidad Carlos III de Madrid, Departamento de Física, Avda de la Universidad 30, 28911-Leganés, Madrid, Spain
[b] Universidad de Castilla-La Mancha, Departamento de Fisica Aplicada and INEI, 13071 Ciudad Real, Spain

ARTICLE INFO

Keywords:
Dispersion Strengthened copper
Powder metallurgy route
Hot rolling
Thermal conductivity of ODS copper

ABSTRACT

Dispersion strengthened copper alloys have been produced by following a powder metallurgy route that have consisted of milling copper and yttrium acetate powders in a planetary ball milling and subsequently sintering by hot isostatic pressing (HIP). In order to increase the degree of densification of the materials, they were subjected to a thermal treatment in vacuum and to a hot rolling process at 1173 K. The decomposition of the yttrium acetate during the thermal treatments resulted in the formation of voids, with a loss of densification that could not be satisfactorily improved with the hot rolling processing. The microstructure and the mechanical and thermal properties of the alloys were analyzed by scanning electron microscopy, electron backscattering diffraction, micro and nanohardness measurements, and compression tests and thermal conductivity measurements, both in the range 300–780 K. The best mechanical properties were obtained for the as-HIP material, with a mean grain size of 0.3 ± 0.3 μm and a yield strength value at room temperature of 520 MPa. In contrast, the material with the highest thermal conductivity for the entire range of temperature was found to be the alloy thermal treated in vacuum at 1273 K and later subjected to the hot rolling processing. The different microstructural characteristics of the alloys such as grain size, defects present in the grains and size of voids seems to be responsible of the differences on their thermal conductivity values.

1. Introduction

Copper-based materials are leading candidates for heat sink components of water-cooled elements of future fusion reactors, as the divertor and blanket for Thermonuclear Experimental Reactor (ITER) [1,2], due to their high thermal conductivity and acceptable mechanical properties at moderate temperatures. Specifically, the precipitation hardened alloy CuCrZr is the candidate for the water-cooled PFCs designs in ITER [3,4].

Although the mechanical properties of CuCrZr below 623 K are acceptable for the ITER requirements, above 673 K, the precipitate coarsening and the matrix recrystallization yield to a deterioration of the mechanical strength. Additionally, if CuCrZr is submitted to irradiation above 573 K, softening of mechanical properties occurs [4,5]. Other important deficiency in CuCrZr that can explain its poor mechanical properties at high temperature, is the lack of precipitates in the grain boundaries. The presence of precipitates in the grain boundaries can prevent the deformation by grain sliding. There are other precipitation hardened alloys, such as Cu-8at%Cr-4at%Nb (GRcop-84) and CuCrNbZr, in which the presence of precipitates in the grain boundaries is possible. GRcop-84 is fabricated by using solidification and powder metallurgy routes, which allows the formation of Cr_2Nb precipitates at the grain boundaries [6]. This alloy exhibits an attractive balance between strength, creep resistance and thermal conductivity, in particular above 673 K. However, its fabrication is relatively expensive, since it is necessary to control the size and distribution of the Cr_2Nb precipitates. CuCrNbZr is also a precipitation hardened alloy which presents Cr_2Nb precipitates at the grain boundaries along with a fine distribution of Cr precipitates in the copper matrix. This alloy shows higher creep strength, higher creep fracture ductility and longer creep life than CuCrZr at 773 K [7,8].

A different strategy for improving the mechanical properties of pure copper is the dispersion of fine hard oxides particles that present a good thermal stability at high temperature, such as Al_2O_3 and Y_2O_3. Dispersion strengthened (DS) copper alloys can be obtained either by internal oxidation or by mechanical alloying. Recently, DS Cu-Y_2O_3 and Cu-Y alloys have been produced by mechanical alloying [9–12]. In general, the mechanical alloying process is the most suitable method for achieving a good dispersion of hard particles in a metallic matrix. However, copper exhibits a high ductility, and cold welding phenomena usually appear during the milling process, originating the agglomeration of the powder particles. This can be avoided by using a process control agent (PCA) as stearic acid [11,12], but in this case, previously to the sintering process, the dispersive agent must be eliminated from

* Corresponding author.
E-mail address: angel.munoz@uc3m.es (A. Muñoz).

https://doi.org/10.1016/j.nme.2020.100754
Received 31 January 2020; Received in revised form 6 May 2020; Accepted 7 May 2020
Available online 16 May 2020

the powder by some thermal treatment. Thus, an interesting and alternative procedure would consist of adding a certain compound that plays the role of a PCA and simultaneously facilitate the formation and dispersion of oxides particles in the copper matrix. A fabrication process of this type has already been checked in the synthesis of Ni/Y_2O_3 nanocomposites [13]. In this study, a similar procedure has been followed, grinding in a planetary ball milling a mixture of copper and yttrium acetate ($Y(CH_3CO)_3{\cdot}4H_2O$) powders in order to obtain DS Cu-Y_2O_3. Previously to the sintering process by high isostatic pressing (HIP), the milled powder was thermal treated in a reducing hydrogen-enriched atmosphere, which resulted in the decomposition of yttrium acetate and the formation of yttrium-enriched particles. The presence of yttrium acetate prevented cold welding phenomena and allowed the formation of the reinforcing particles, but gave place to the formation of voids after the sintering process. In order to increase the densification degree, in this research work DS Cu-Y_2O_3 alloys produced following this new fabrication method have been subjected to hot rolling at 1173 K, with reductions of about 29% and 39%. The microstructure of the deformed alloys has been analyzed employing scanning electron microscopy and electron backscatter diffraction measurements and the mechanical properties have been studied by nanoindentation measurements at room temperature and compression tests performed from room temperature up to 773 K.

2. Experimental procedure

A blend of Cu (99% purity) and $Y(OOCCH_3)_3{\cdot}4H_2O$ (99.9% purity) powders with a nominal composition of 97 wt% of Cu and 3 wt% of Y $(OOCCH_3)_3{\cdot}4H_2O$ was grinded into a planetary ball milling during 72 h at 150 rpm under a high purity argon atmosphere. The grinding media were 5 mm Ø Cr steel balls and the ball to powder ratio was 7:1. Later, the powders were thermal treated at 1173 K during 4 h under a flowing reducing gas of composition Ar-10Vol%H_2. Subsequently, the powder was encapsulated into a steel can and a degassing process in vacuum during 24 h at 573 K was performed. Finally, the powders were sintered by HIP at 1173 K during 3 h under a 179 MPa pressure. Following this procedure, two batches were obtained, the first one was hot rolled (HR) at 1173 K with a size reduction of 29% and was denoted as HIP + HR. The second batch was submitted to a thermal treatment at 1273 K in vacuum, and later hot rolled at 1173 K to a reduction of 39%. This second batch was named HIP + TTV + HR.

X-Ray diffraction patterns were acquired along the different steps of the fabrication process for analyzing the presence of impurities. The degree of consolidation of the alloys was determined with a He Ultrapycnometer and also by using the Archimedes principle. The microstructure was analyzed with a high resolution scanning microscope (SEM) FE-SEM FEI TENEO, accelerating voltage 0.2–30 kV, equipped with an energy dispersive X-Ray spectroscopy (EDAX) detector. The EBSD patterns were obtained with a scanning microscope SEM-FEG JEOL JSM 6500F, accelerating voltage 0.1–30 kV, equipped with an EBSD detector. The EBSD images were analyzed using the MTexv3.2.5 data analysis software [14]. In order to discriminate the grain boundaries, it was considered a crystallographic misorientation larger than 5° between adjacent crystalline domains. The experimental grain size distributions were evaluated from the ECC images using the Jhonson–Saltykov stereological method. With this method, it is possible to obtain the spatial grain size distribution of a 3D microstructure from 2D grain size measurements [15].

The mechanical behavior was studied by compression tests in the temperature range 300–773 K at a strain rate of $1.0 \times 10^{-4}\ s^{-1}$, and by Vickers-microhardness and Berkovich-nanohardness measurements at room temperature. The microhardness measurements were carried out on applying a 9.81 N load during 20 s. Nanohardness maps were obtained from a square array of 900 indentations using a load of 53 mN and a spacing of 3 μm. For the compression tests, cylindrical samples 9 mm height and 5 mm diameter were used.

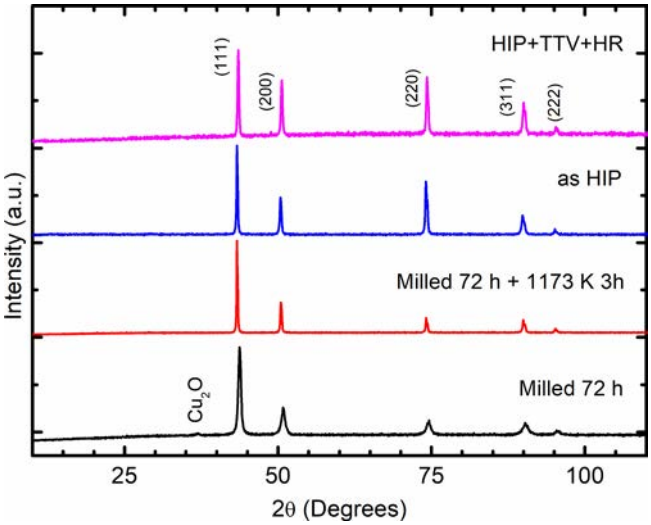

Fig. 1. X-Ray diffraction patterns of the alloy HIP + TTV + HR along the different steps of the fabrication route.

The thermal properties of the alloys have been inferred from the measurements of the thermal diffusivity, α, and the specific heat, Cp in the temperature range 323–773 K. The thermal conductivity, λ, was determined from the expression: $\lambda = \alpha{\cdot}C_p{\cdot}\rho$ where ρ denotes the density. The thermal diffusivities were measured by the laser flash method in a LFA 1000 instrument under an argon atmosphere. The sample size was 9.5 × 9.5 × 1 mm^3. The specific heat measurements were performed with a Netzsch Jupiter DSC 404 differential scanning calorimeter in Pt crucibles (scan rate 20 K min^{-1}) under helium atmosphere on disc-shaped samples with a diameter of 5 mm and 1 mm of thickness. A single-crystalline sapphire sample was used as the reference material.

3. Results and discussion

3.1. Microstructure

The X-Ray diffraction patterns of the alloy HIP + TTV + HR along the different steps of the fabrication route are shown in Fig. 1. Except for the X-Ray pattern corresponding to the powder after 72 h milling, only the Bragg peaks associated to the copper are observed. The extra peak observed in the 72 h milled powder is related to the strongest Bragg peak of Cu_2O. During the milling process, the dehydratation of the yttrium acetate tetrahydrate can form some copper oxides, in particular Cu_2O, since its formation enthalpy is more negative (−170.71 kJ/mol) than that of CuO (−150.06 kJ/mol) [16]. This oxide is not observed in the X-ray pattern after the thermal treatment of the powder in a hydrogen-rich atmosphere, what indicates that this kind of atmosphere may facilitate the decomposition of some products involved in the disintegration of the yttrium acetate that lead to the formation of copper oxides. On the other hand, for the HIPed materials, no changes are observed in the relative intensities of the Cu Bragg peaks, indicating that there is not an appreciable macrotexture even after the hot rolling process.

The densities of the alloys after HIP and after the HR process are shown in Table 1. In order to establish the degree of densification, the theoretical value of the density of the alloy must be evaluated. This theoretical value has been determined by using the phases rule and assuming that all the Y present in the yttrium acetate transforms into Y_2O_3, so the nominal composition of the alloy would be Cu-1 wt%Y_2O_3. Thus, considering 8.960 and 5.01 g cm^{-3} as the densities of Cu and Y_2O_3, respectively, a theoretical value of 8.889 g cm^{-3} is calculated. After HIP, the degree of densification is relatively low, only 94.15%, and the hot rolled process reduces the degree of densification (see

Table 1
Density, degree of densification and Vickers-microhardness of the DS Cu alloys.

Sample	Density (g/cm^3)	Densification (%)	Vickers Microhardness (GPa)
as-HIP	8.370 ± 0.003	94.15 ± 0.03	1.3 ± 0.2
HIP + TTV	6.190 ± 0.002	69.63 ± 0.02	0.55 ± 0.01
HIP + HR	7.364 ± 0.002	82.84 ± 0.02	0.89 ± 0.06
HIP + TTV + HR	7.793 ± 0.002	87.66 ± 0.02	0.89 ± 0.06

Table 1). The decomposition of the yttrium acetate during the thermal treatment under a hydrogen atmosphere can originate some gas bubbles that remain trapped in the powder particles. During the sintering process by HIP and the posterior hot rolling process, these gas bubbles can give place to the formation of voids, as they have been observed by scanning electron microscopy during the microstructure analysis. As it will be shown in the analysis of the SEM micrographs, the present rolling process is efficient in the closure of the sub-micrometer pores but not in eliminating the cavities of micrometer size, causing their coalescence.

The microstructure of the alloys, observed by SEM, is shown in Fig. 2. After HIP (Fig. 2a), the microstructure consists of equiaxed grains with sizes both in the micrometric and submicrometric range. According to Fig. 2a, most of the micrometric grains contain twins, which correspond to annealing twins that were formed during the recrystallization process that takes place during the sintering by HIP. Additionally, a great number of submicrometric pores are observed, which are located both in the grain boundaries and inside the large grains. Voids with a micrometric size are also observed. The most important effect induced by the posterior thermal treatment at 1273 K in vacuum is the appearance of more voids (Fig. 2b), so it is inferred that in the sintered alloy remains some trapped gas, which is released during the thermal treatment in vacuum, giving place to new voids. The effect of the hot rolling treatment in the alloys is shown in Fig. 2c and d. Many of the pores present within the grains appear to be closed by the rolling process. However, as regarding the micrometric voids, although their shape has changed, they could not be closed. On the other hand, cracks are observed in the regions with submicrometric grains. These cracks could have appeared as a consequence of the coalescence of the small pores located at the grain boundaries. These results are coherent with the decrease of the degree of densification observed in the density measurements. Therefore, greater reductions in the hot rolling process would be necessary in order to achieve an effective increase of the degree of densification.

3.2. Electron backscattering diffraction results

The orientation image micrographs (OIMs) obtained from the EBSD analysis are shown in Figs. 3 and 4. In Fig. 3a and c the pictures corresponding to the HIP and HIP + HR alloys are compared. The hot rolling process originates an increase in the average grain size, from 0.3 ± 0.3 to 1.0 ± 0.8 μm, as Fig. 3b evidences (see Table 2). Furthermore, there is also an increase in the percentage of twins which are observed inside the grains, which indicates that the rolling process promotes the recrystallization phenomena. On the other hand, the grain misorientations of the as-HIP and HIP + HR alloys are compared in Fig. 3d. According to the figure, both distributions are similar to the Mackenzie one, indicating that the macrotexture is negligible in both alloys. There is an exception at 60°, which corresponds to the primary copper annealing twins 60° ⟨1 1 1⟩ . Fig. 4 shows the effect on the microstructure of carrying out the thermal treatment before the hot rolling process. The only remarkable point is that the average grain size decreases to ~0.7 μm. Regarding the average grain size, twin percentage and texture, there are negligible differences between the longitudinal and transversal sections, as shown in Table 2.

3.3. Mechanical properties

The Vickers-microhardness values of the alloys measured at room temperature are displayed in Table 1. The greatest value, 1.3 ± 0.2 GPa, was found for the as-HIP alloy. As this value is greater than the corresponding to pure copper, 0.369 GPa [17], it indicates that a reinforcement of the copper matrix has taken place. The thermal treatment considerably lowered the microhardness value of the alloy, in agreement with the increase in the number of voids observed by SEM and the density measurements. Also, the values of the microhardness measured for the rolling samples, i.e. HIP + HR and HIP + TTV + HR, are in accord with the SEM observations. Whereas the rolling of the HIP + TTV sample induces some closure of the voids and pores with the consequent improvement of the microhardness, the hot rolling of the

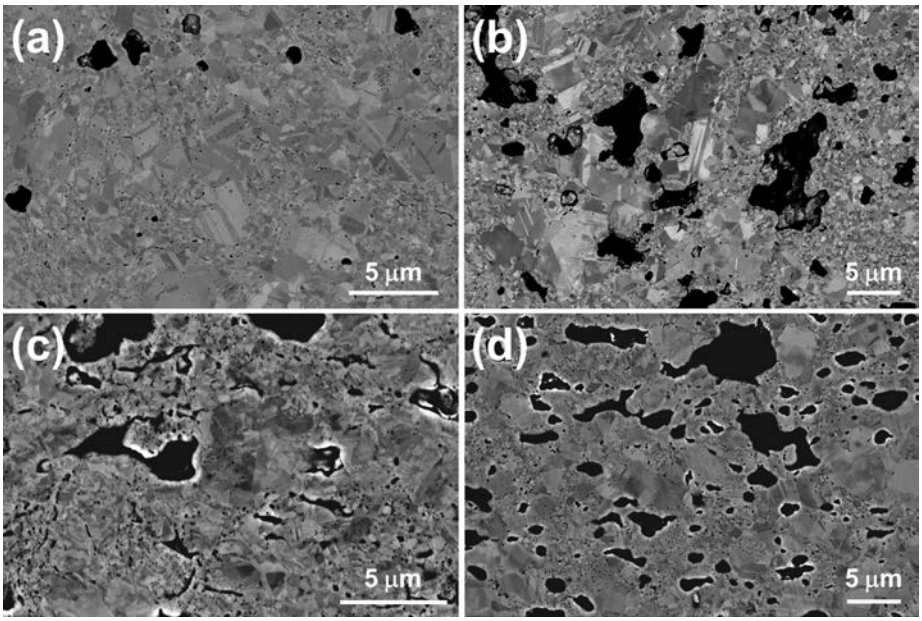

Fig. 2. Micrographs of the microstructure obtained by SEM. (a) After sintering by HIP; (b) After sintering plus thermal treatment in vacuum (HIP + TTV); (c) After sintering plus hot rolling (HIP + HR); (d) After sintering plus thermal treatment in vacuum and posterior hot rolling HIP + TTV + HR.

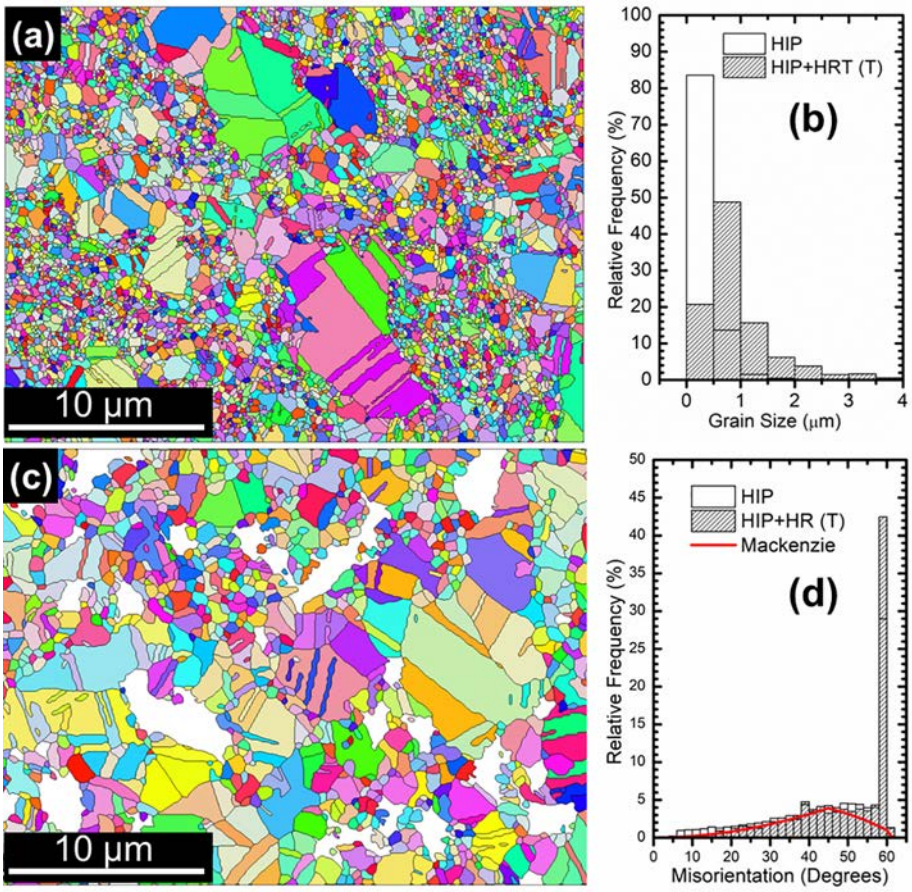

Fig. 3. (a) and (c) Orientation image micrographs for as-HIP and HIP + HR (transversal direction) materials, respectively; (b) Grain size distributions; (d) Grain size misorientation and Mackenzie's misorientation distributions.

as-HIP sample leads to the detriment of the microhardness, since a great number of voids are being formed during the thermomechanical process.

Contour maps showing the nanohardness distributions along with the corresponding histograms are depicted in Figs. 5–7 for the different alloys. The nanohardness maps were obtained from 100 μm × 100 μm areas, which contain a great number of grains, and allow to visualize the effect of the voids on the homogeneity of the hardness. As it can be appreciated in the figures, the nanohardness is not uniform, in particular, the regions closer to the voids exhibit a smaller value. As it can be observed in Fig. 5, the as-HIP alloy presents the lower dispersion of the nanohardness value, with an average value around 2.5 GPa. When this alloy is subjected to the hot rolling process, the histogram of the distribution (Fig. 6) shows much more dispersion, demonstrating the effect of the formation of a great number of voids and pores during the thermomechanical process. Also, the nanohardness map for the HIP + TTV + HR alloy (Fig. 7) illustrates the influence of performing a vacuum thermal treatment before the hot rolling processing, as it evidences that almost all voids are formed during the thermal treatment and that the hot rolling is able to close a considerable number of them. Additionally, if the right parts of the histogram of the three samples are compared, a correlation between the nanohardness maximum values and the grain size is found.

The thermal evolution of the yield strength values of the different alloys obtained from the compression tests performed from RT to 753 K are shown in Fig. 8. The values are compared with the yield strength of pure copper found in the bibliography [18]. Up to 473 K, despite the presence of pores and voids, the yield strength of the as-HIP and HIP + TTV + HR materials exhibit higher values than pure copper. Above 473 K, the yield strength suffers an important decrease, retaining the as-HIP sample values very close to those of pure copper. This diminution would be due to the appearance of dynamic recovery associated to the recrystallization phenomenon.

3.4. Thermal conductivity measurements

The experimental values of the thermal diffusivity, α, and specific heat, $C_{p,}$ versus temperature for the different alloys are displayed in Figs. 9 and 10, respectively. The thermal conductivity obtained from the expression $\lambda = \alpha \cdot C_p \cdot \rho$ is presented in Fig. 11. The thermal diffusivity is a property that describes the rate of heat transfer inside the material. It was found to be nearly constant for all the alloys in this temperature range, being the as-HIP alloy the one with the smaller thermal diffusivity values. On the other hand, the specific heat represents the ability of the material for storing thermal energy. In a metal, both the electrons and the lattice vibration contribute to the specific heat, but above the Debye temperature (~343 K for pure copper [19]), the lattice contribution hardly depends on temperature. According to Fig. 10, the specific heat of the as-HIP material is nearly constant with temperature, however, the HIP + HR and HIP + TTV + HR materials seems to exhibit a linear dependence. Therefore, the temperature dependence observed in these last alloys should be due to the electron contributions, which play an important role. Fig. 11 shows that the HIP + TTV + HR material presents the highest thermal conductivity values in the whole range of temperatures and the as-HIP material the lowest for temperatures above 420 K. According to the measurements of the density, the degree of densification is greater in the as HIP material, so it would be expected that this material exhibits higher thermal conductivity than the other materials. However, the thermal conductivity also depends on different

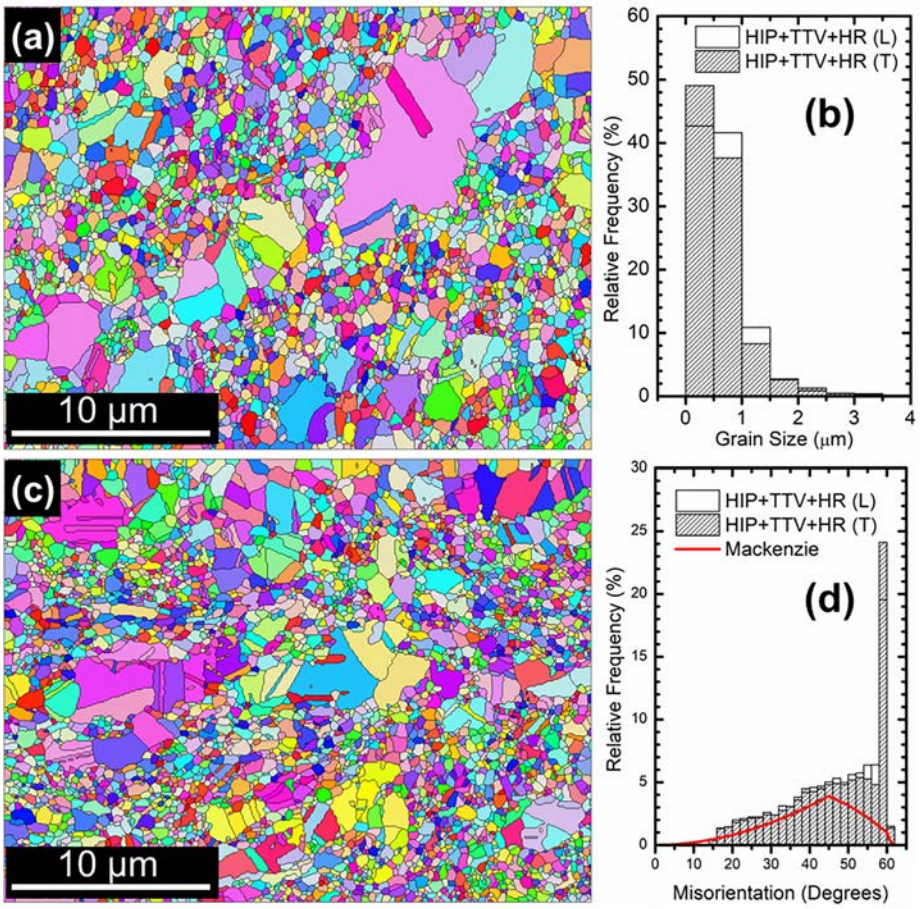

Fig. 4. Results of the EBSD analysis for the HIP + TTV + HR material. (a) and (c) Orientation image micrographs along the longitudinal (L) and transversal (T) directions, respectively; (b) Grain size distributions; (d) Grain size misorientation and Mackenzie's misorientation distributions.

Table 2
Grain sizes and twin percentage obtained from the EBSD analysis.

Sample	Grain size (μm)	Twins percentage (%)
As-HIP	0.3 ± 0.3	62.4
HIP + HR (T)	1.00 ± 0.08	74.9
HIP + TTV + HR (L)	0.7 ± 0.5	62.6
HIP + TTV + HR (T)	0.6 ± 0.5	57.5

microstructural parameters such as grain size and shape, point defects, dislocations, impurities, voids, etc., as these factors modify, among others, the phonon scattering and the grain boundary scattering and therefore, the mean free path and the thermal conductivity [20,21]. In the case of the HIP + HR material, the hot rolling process originated an increase in the grain size, with the subsequent diminution of the grain boundaries, what decreases the interface scattering on electrons. On the other hand, the dynamic recrystallization that took place during the rolling process decreased the number of defects present in the grains, having these two factors a notable influence in the increase of the thermal conductivity. Additionally, the thermal conductivity increases when voids move towards surfaces, or small voids collapse to form large pores [22], as it occurs in the thermomechanical processed samples. For the HIP + TTV + HR material, with a grain size lower than HIP + HR but higher than the as-HIP alloy, the great increase of the degree of densification with respect to the as HIP + HR alloy has an important contribution in its elevated thermal conductivity.

Let us point out that these alloys exhibit lower thermal conductivity values than the reference material for ITER, CuCrZr, and pure copper,

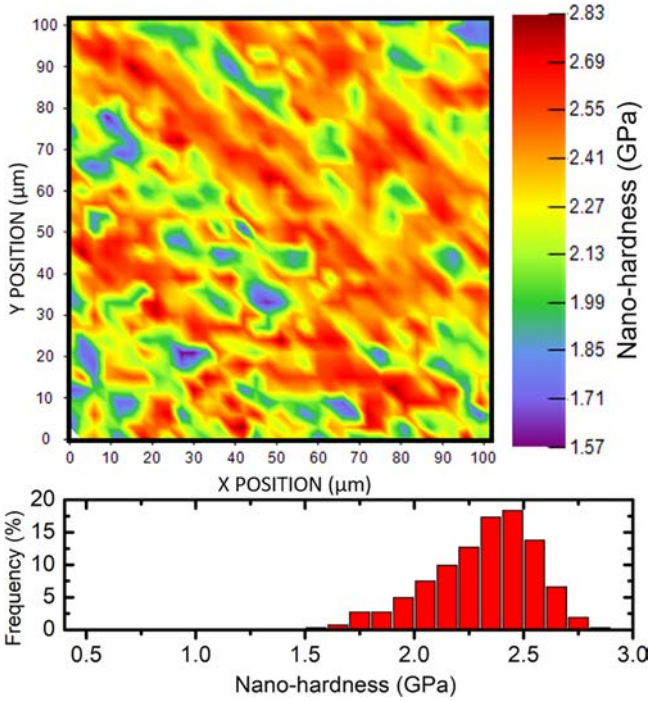

Fig. 5. Nanohardness contour map and corresponding histogram for the as-HIP alloy.

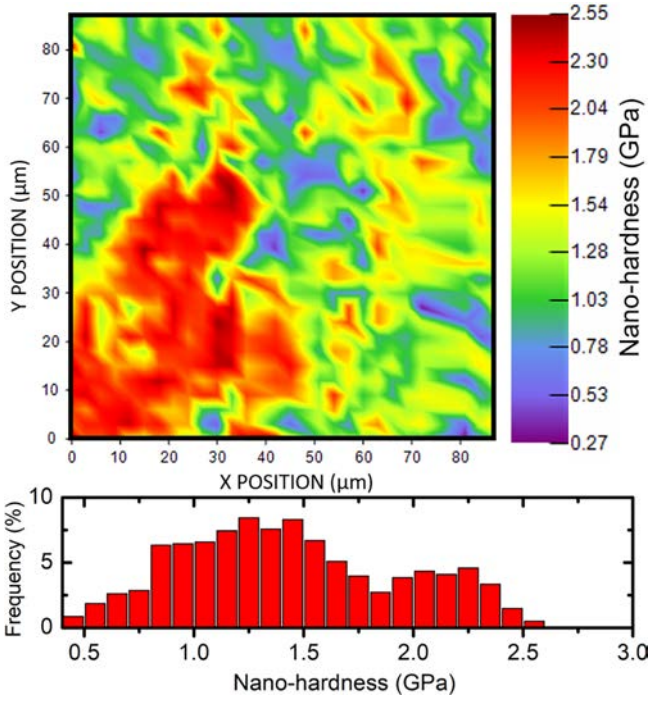

Fig. 6. Nanohardness contour map and corresponding histogram for the HIP + HR alloy.

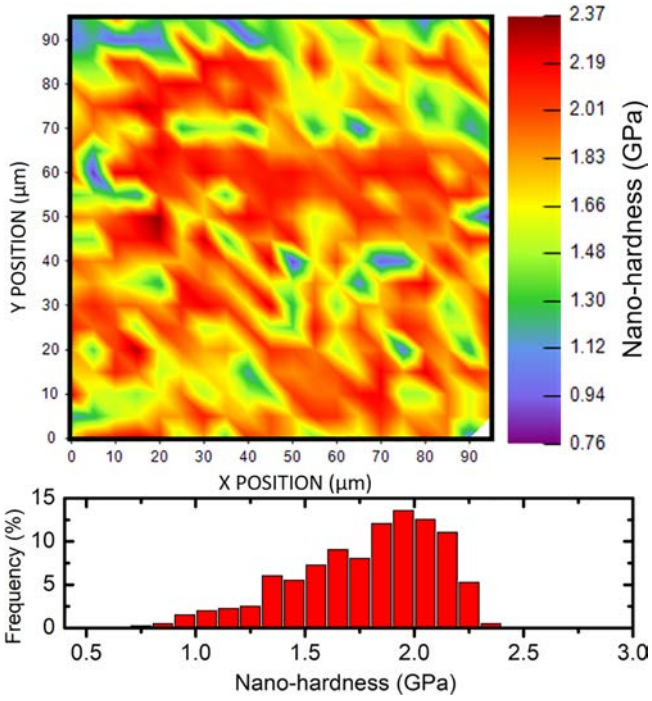

Fig. 7. Nanohardness contour map and corresponding histogram for the HIP + TTV + HR alloy.

whose thermal conductivities are ~350 Wm^{-1} K^{-1} [23] and ~390 Wm^{-1} K^{-1}, respectively.

4. Conclusions

DS Cu-Y alloys have been produced by following a powder metallurgy route that has consisted of milling copper and yttrium acetate ($Y(CH_3CO)_3{\cdot}4H_2O$) powders in a planetary ball milling and

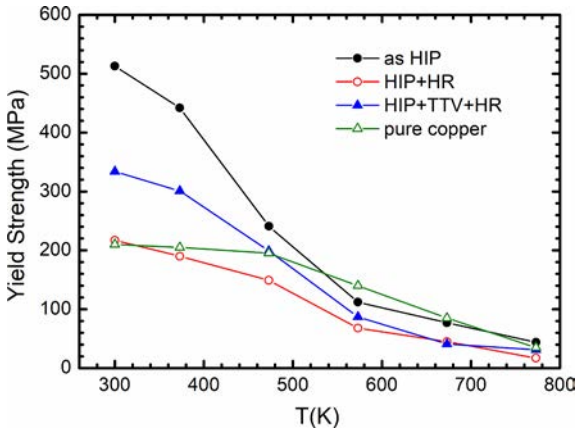

Fig. 8. Thermal evolution of the yield strength of the different materials. The thermal evolution for pure copper is also included.

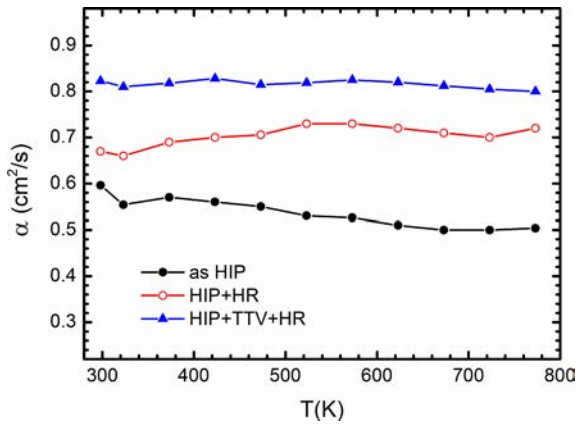

Fig. 9. Thermal diffusivity of the alloys in the temperature range 300–773 K.

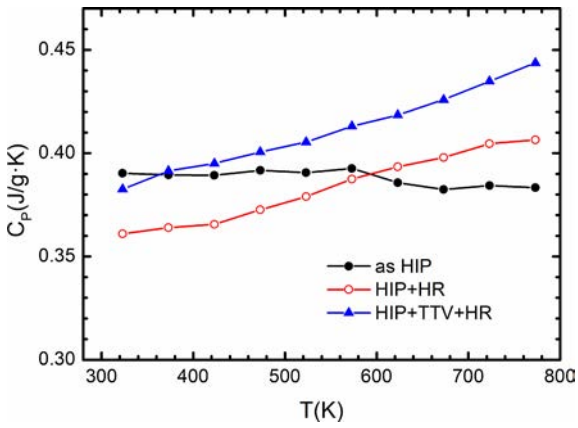

Fig. 10. Heat capacity of the alloys in the temperature range 300–773 K.

subsequently sintering by hot isostatic pressing. In order to increase the degree of densification, the materials have been subjected to a hot rolling process at 1173 K. The conclusions derived from this research work are the following ones:

1. The degree of densification of the as-HIP material is only 94.15%. Voids of different sizes have being observed in the microstructure. The thermal treatment performed in the powder under a hydrogen atmosphere for transforming the yttrium acetate into Y_2O_3 can originate some gas bubbles that remain trapped in the powder particles. The release of this gas during the HIP process and

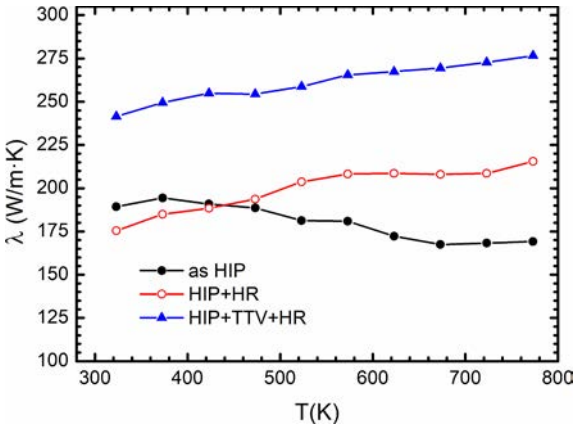

Fig. 11. Thermal conductivity of the alloys in the temperature interval 300–773 K.

posterior thermal treatments would give place to the formation of the voids.

2. The hot rolling process carried out at 1173 K is able to close the submicrometric pores which are present inside the grains. However, higher reductions would be necessary in order to achieve a satisfactory closure of the voids. A thermal treatment in vacuum previous to the hot rolling process is beneficial for increasing the degree of densification.
3. The as-HIP material presents equiaxed grains with sizes in the micro and submicro ranges. Many micrometric grains contain annealing twins formed during the recrystallization process that takes place during the sintering by HIP.
4. The EBSD analysis has shown that, in the as-HIP samples, hot rolling process at 1173 K originates an increase in the average grain size. The average grain size goes from 0.3 ± 0.3 for the as HIP material to 1.0 ± 0.8 μm for the HIP + HR one. Furthermore, the recrystallization phenomena that also appear during the hot rolling process originate an increase in the twin percentage. On the other hand, the hot rolling process does not give place to an appreciable macrotexture.
5. The compression tests performed from RT to 773 K have concluded that the yield strength of the as HIP material exhibits the greatest value up to 473 K due to its higher densification. After 473 K, it is observed an important decrease in the yield strength for all the materials which is due to the appearance of a dynamic recovery associated to recrystallization phenomenon. The micro and nanohardness measurements performed in the as-HIP sample indicate a reinforcement of the copper matrix.
6. The thermal conductivity measurements have shown that the HIP + TTV + HR material exhibits the high thermal conductivity in the temperature range 300–773 K. The as HIP material is the alloy with lower thermal conductivity values. Although the thermal treatment in vacuum and the rolling process do not improve degree of densification, there are certain microstructural parameters, such as less grain boundaries and less dislocations, that improve during this process, which originate an amelioration of the thermal conductivity.

The method described in this research work for obtaining copper reinforced with Y_2O_3 particles is very promising, except by the appearance of voids that originate an important deterioration of the mechanical properties. The origin of the voids lies in the gas bubbles which are formed during the thermal treatment carried out to the powder, in order to remove the rests of the Yttrium acetate. To avoid the bubbles formation, the thermal treatment might be performed at a higher temperature and under an atmosphere more hydrogen-enriched. However, it would yield to the sintering of the powder, probably with a densification below 90 %, what would made HIP not be the suitable method for the final sample consolidation. Nevertheless, in this case, extrusion at high temperature, around 1173 K, might be a suitable method for the alloy sintering.

CRediT authorship contribution statement

A. Muñoz: Conceptualization, Methodology, Investigation, Writing - original draft, Visualization, Supervision, Project administration, Funding acquisition. **B. Savoini:** Conceptualization, Methodology, Investigation, Writing - review & editing, Supervision, Funding acquisition. **M.A. Monge:** Conceptualization, Methodology, Investigation, Software, Formal analysis, Supervision, Funding acquisition. **O.J. Dura:** Investigation.

Declaration of Competing Interest

The authors declare that they have no known competing financial interests or personal relationships that could have appeared to influence the work reported in this paper.

Acknowledgements

The present work has been supported by the Ministerio de Economía y Competitividad of Spain (ENE2015-70300-C3-2-R MINECO/FEDER) and by the Regional Government of Madrid through the program TECHNOFUSIÓN(III)CM (S2018/EMT-4437). We are very grateful to Dr. Fernando Carreño and to the technicians Carmen Peña and Miguel Angel Acedo of the CENIM (CSIC-Madrid) for their expertise and assistance in the hot rolling facilities. We thank also our colleagues of the CENIM (CSIC-Madrid) for the EBSD measurements.

References

[1] S.J. Zinkle, Applicability of copper alloys for DEMO high heat flux components, Phys. Scr. (2016) 10. T167, 014004.
[2] J.H. You, Copper matrix composites as heat sink materials for water-cooled divertor target, Nucl. Mater. Energy 5 (2015) 7–18.
[3] S.A. Fabritsiev, S.J. Zinkle, B.N. Singh, Evaluation of copper alloys for fusion reactor divertor and first wall components, J. Nucl. Mater. 233–237 (1996) 127–137.
[4] D. Stork, et al., Materials R&D for a timely DEMO: key findings and recommedations of the EU Roadmap Materials Assessment Group, Fusion Eng. Des. 89 (2014) 1586–1594.
[5] M. Li, S.J. Zinkle, Physical and mechanical properties of copper and copper alloys, Compr. Nucl. Mater. 4 (2012) 667–690.
[6] H.C. de Groh, D.L. Ellis, W.S. Loewenthal, Comparison of GRCop-84 to other Cu alloys with high thermal conductivities, J. Mater. Eng. Perform. 17 (2008) 594–606.
[7] Y. Yang, L. Wang, L. Snead, S.J. Zinkle, Development of novel Cu-Cr-Nb-Zr alloys with the aid of computational thermodynamics, Mater. Des. 156 (2018) 370–380.
[8] L. Wang, C. Zheng, B. Kombaiah, L. Tan, D.J. Sprouster, L.L. Snead, S.J. Zinkle, Y. Yang, Contrasting roles of Laves Cr_2Nb precipitates on the creep properties of novel CuCrNbZr alloys, Mater. Sci. Eng. A 779 (2020) 139110.
[9] G. Carro, A. Muñoz, M.A. Monge, B. Savoini, R. Pareja, C. Ballesteros, P. Adeva, Fabrication and characterization of Y_2O_3 dispersion strengthened copper alloys, J. Nucl. Mater. 455 (2014) 655–659.
[10] G. Carro, A. Muñoz, B. Savoini, M.A. Monge, R. Pareja, Processing, microstructure and mechanical characterization of dispersion strengthened Cu-1%Y, Fusion Eng. Des. 138 (2019) 321–331.
[11] S.M.S. Aghamiri, N. Oono, S. Ukai, R. Kasada, H. Noto, Y. Hishinuma, T. Muroga, Microstructure and Mechanical properties of mechanicallyalloyed ODS copper alloy for fusion material application, Nucl. Mater. Energy 15 (2018) 17–22.
[12] D. Zhou, H. Geng, W. Zeng, D. Zheng, H. Pan, C. Kong, P. Munroe, G. Sha, C. Suryanarayana, D. Zhang, High temperature stabilization of a nanostructured Cu-Y2O3 composite through microalloying with Ti, Mater. Sci. Eng. A 712 (2018) 80–87.
[13] K. Byungchul, J. Jinsung, K. Tae Kyu, A. Jung-Ho, Synthesis and properties of Ni/Y_2O_3 nanocomposites, Rev. Adv. Mater. Sci. 28 (2011) 166–170.
[14] F. Bachmann, R. Hielscher, H. Schaeben, Grain detection from 2d and 3d EBSD data Specification of the MTEX algorithm, Ultramicroscopy 111 (2011) 1720–1733.
[15] Y.H. Xu, H.C. Pitot, An improved stereologic method for three-dimensional estimation of particle size distribution from observations in two dimensions and its application, Comput. Methods Programs Biomed. 72 (2003) 1–20.
[16] M.W. Chase, Jr., NIST-JANAF Themochemical Tables, Fourth Edition, J. Phys. Chem. Ref. Data, Monograph 9 (1998) 1–1951.
[17] B.N. Singh, A. Horsewell, P. Toft, D.J. Edwards, Temperature and dose

dependencies of microstructure and hardness of neutron irradiated OFHC copper, J. Nucl. Mater. 224 (1995) 131–140.
[18] T.J. Miller, S.J. Zinkle, B.A. Chin, Strength and fatigue of dispersion-strengthened copper, J. Nucl. Mater. 179–181 (1991) 263–266.
[19] Kittel Charles, Introduction to Solid State Physics, John Wiley & Sons, 2004.
[20] O. Kahveci, E. Çadirli, M. Arı, H. Tecer, M. Gündüz, Measurement and prediction of the thermal and electrical conductivity of Al-Zr overhead line conductors at elevated temperatures, Mater. Res. 22 (1) (2018) 20180513.
[21] M. Schrade, K. Berland, S.N.H. Eliassen, et al., The role of grain boundary scattering in reducing the thermal conductivity of polycrystalline XNiSn (X = Hf, Zr, Ti) half-Heusler alloys, Sci. Rep. 7 (2017) 13760.
[22] X.W. Zhou, R.E. Jones, Effects of nano-void density, size and spatial population on thermal conductivity: a case study of GaN crystal, J. Phys. Condens. Matter 24 (2012) 325804.
[23] G. Purcek, H. Yanar, M. Demirtasb, Y. Alemdag, D.V. Shanginac, S.V. Dobatkin, Optimization of strength, ductility and electrical conductivity of Cu–Cr–Zr alloy by combining multi-route ECAP and aging, Mater. Sci. Eng. A 649 (2016) 114–122.